Novel Low Melting Point Alloy-Loaded Polymer Composite. II. Resistivity–Temperature Behavior

XIANGWU ZHANG,[1] YI PAN,[1] LIE SHEN,[1] XIAOSU YI[2]

[1] Department of Polymer Science and Engineering, Zhejiang University, Hangzhou 310027, People's Republic of China

[2] National Key Laboratory of Advanced Composites, P.O. Box 81-3, Beijing 100095, People's Republic of China

Received 12 May 1999; accepted 22 August 1999

ABSTRACT: The effect of temperature on the resistivity of Sn–Pb alloy-loaded PS composites was studied. The composites have distinctive positive temperature coefficient (PTC) effects with high PTC intensity, abrupt PTC transition, etc. According to SEM and EDAX analyses, the morphology of the alloy particles in the composites remained unchanged as the temperature reached the melting point of the alloy, while the alloy dispersion changed. The viscosity of the composites decreased sharply when the alloy melted. © 2000 John Wiley & Sons, Inc. J Appl Polym Sci 77: 756–763, 2000

Key words: low melting point alloy; composite; positive temperature coefficient; surface energy; viscosity

INTRODUCTION

Metal-loaded polymer composites have been studied as electrically conductive materials for many years.[1–5] However, low melting point alloy-loaded polymers are still a new family of conductive polymer matrix composites.[6,7] The morphology of fillers can be greatly varied to, for example, fiber or flake dispersion *in situ* during processing, depending on the processing conditions, mainly the processing temperature. Upon filler dispersion, low room-temperature resistivity, excellent processability, and a special positive temperature coefficient (PTC) effect of the resistance can also be obtained. Therefore, the influence of low melting point alloy on the properties of composites is of great importance from both scientific and engineering points of view.

In the present article, we first studied the resistivity–temperature behavior of low melting point alloy-loaded polymer composites and then tried to explain the result by analyzing the alloy particle dispersion with the digital image analysis (DIA)[8] method. The origin of the PTC effect was also investigated from both thermodynamic and dynamics points of view.

EXPERIMENTAL

Materials

The low melting point alloy used in this study was the Sn–Pb alloy. It was powdered solder of composition 60 wt % Sn, 40 wt % Pb provided by the Institute of Powder Metallurgy at the Zhongnan Technology University of China. The melting temperature range of the alloy is approximately from 183 to 188°C according to the phase diagram, and the mean particle size is about 11 μm. The polymer powder used was polystyrene (PS) with a melting index of 6–10 g/10 min.

Preparations of Composites

The Sn–Pb alloy and PS mixtures, which varied only in the Sn–Pb alloy concentration, were mixed

Correspondence to: X. W. Zhang.

Contract grant sponsor: National Nature Science Foundation of Chinaact grant number: 59683003

Journal of Applied Polymer Science, Vol. 77, 756–763 (2000)

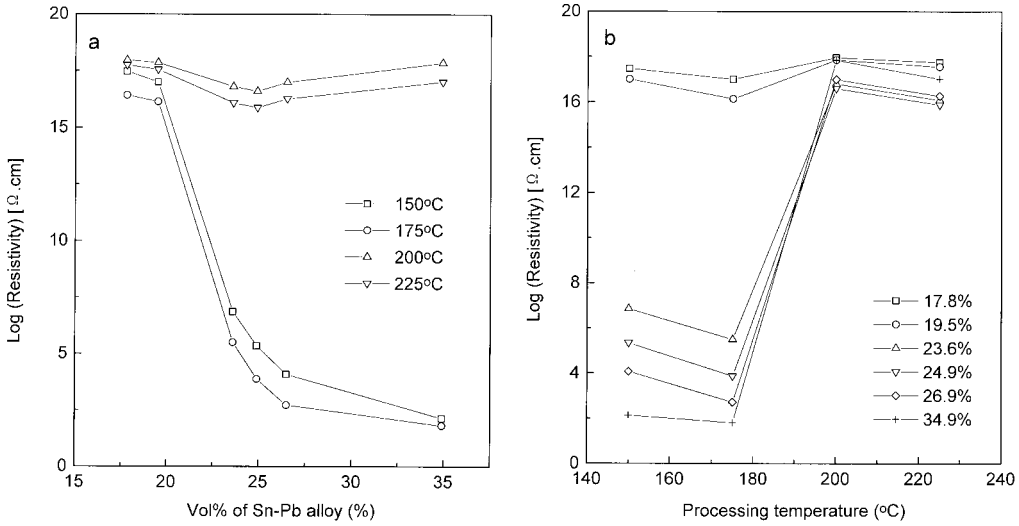

Figure 1 (a) Room-temperature resistivity as a function of the alloy volume fraction for the composites processed at different temperatures. (b) Room-temperature resistivity as a function of the processing temperature for the composites differently loaded.

in a satellite ball mill (QM-1SP) at 200 rpm for 11 h. Then, the powder mixtures were hot-pressed in a matched metal die at various temperatures for 20 min to form the samples.

Measurements

Resistivity

The resistivity of the samples varied over a wide range from 1 to 10^{18} Ωcm. High-resistivity samples were measured on a ZC36 high-resistance electrometer, while low-resistivity samples were measured on an M890D digital electrometer.

The resistivity–temperature curve was obtained using a resistivity–temperature tester that was designed by our laboratory, and the sample size was 1.5 × 1.5 × 0.1 cm. The heating rate adopted was 1.5°C/min.

SEM and EDAX

The SEM used in the study was an S-570 scanning electron microscope with a fairly stable electron-beam intensity. The EDAX used was a PV9900 energy-dispersive analyzing X-ray spectrometer that contained software for X-ray imaging.

Rheological Measurements

Rheological measurements were undertaken on a capillary rheometer (XLY-1), and a capillary of 1 mm in diameter with an aspect ratio $L/D = 40$ was selected for the measurements. The wall shear stress ranged from 18,375 to 183,750 Pa for all the measurements.

RESULTS AND DISCUSSION

Room-Temperature Resistivity

The room-temperature resistivity against the volume fraction of the Sn–Pb alloy is plotted in Figure 1(a). The resistivity did not change much for the composites processed (hot-pressed) at a temperature higher than the melting point of the alloy. However, when the composites were processed at a temperature lower than the melting point, such as 150 and 175°C, the resistivity decreased sharply at about 20 vol %. At an average fraction of 23 vol %, the composite changes from a conductor to an insulator, and this point is usually defined as the critical threshold.

To further investigate the effect of processing temperature on the resistivity, variations of the room-temperature resistivity as a function of the processing temperature at different alloy loadings are plotted in Figure 1(b), which is a direct translation of Figure 1(a). When the alloy filler volume fraction is higher than 23.6 vol % (critical threshold), the room-temperature resistivity increases abruptly from a low value to a value orders of magnitude higher at the processing temperature between 180 and 200°C, corresponding to the melting range of the alloy. The resistivity incre-

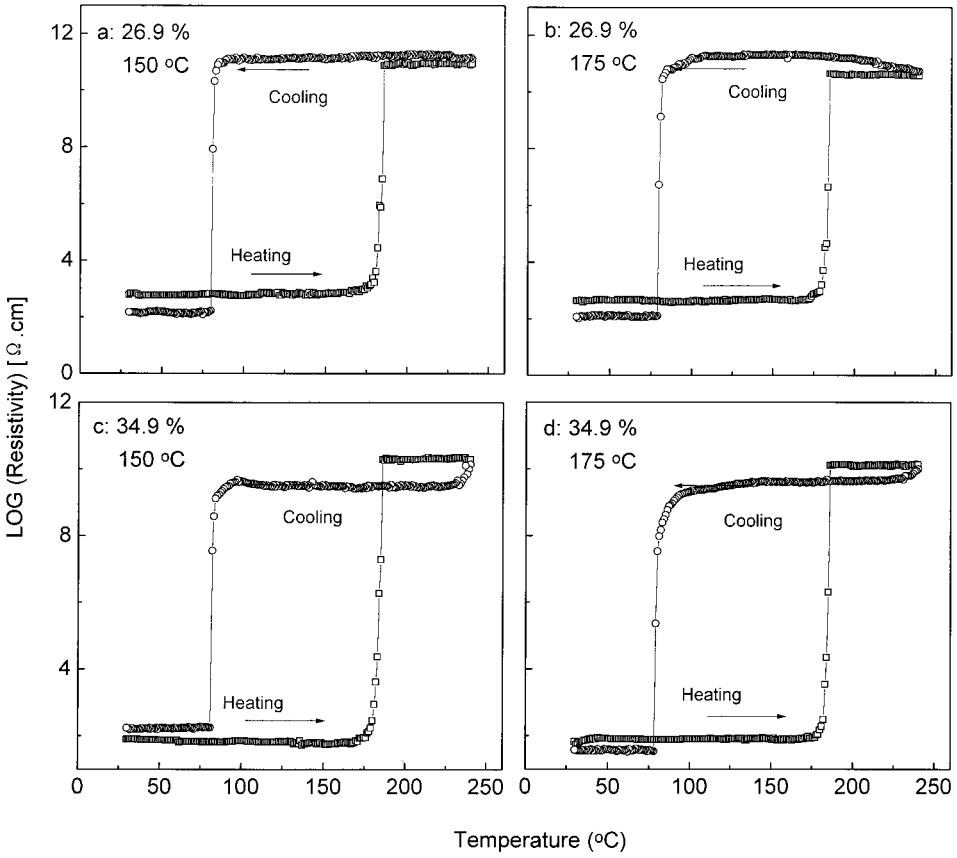

Figure 2 Resistivity–temperature curves for composites differently loaded and processed at various temperatures: (□) heating curves; (○) cooling curves.

ment also was found to increase with increase of the alloy volume fraction, and the largest increment is of 16 orders of magnitude when the alloy volume fraction is the largest (34.9 vol %) of this study.

Resistivity–Temperature Behavior

The resistivity–temperature behavior was measured on the composites loaded with a volume fraction higher than the threshold, and distinctive PTC effects were found (Fig. 2). For all the composites hot-pressed at temperatures of 150 and 175°C, the PTC transition temperature was always in the region of 183–188°C, which is the same as the melting range of the alloy. Therefore, the origin of the PTC effects for the Sn–Pb alloy-loaded PS is the state change of the alloy fillers instead of other changes of the polymer matrix. Furthermore, the PTC transition is very steep compared with the carbon black-loaded polyethylene.[9–11]

The cooling curves are also plotted in Figure 2; it can be seen that the PTC effect of the Sn–Pb alloy-loaded PS is reversible. However, the insulator-to-conductor transition during cooling takes place at the temperature of about 80°C, about 100°C lower than the temperature of the conductor-to-insulator transition during heating. The reason why the transition temperatures are different is not understood by the authors.

The PTC intensity is defined as

$$I_{\mathrm{PTC}} = \log\left(\frac{\rho}{\rho_0}\right) \tag{1}$$

where ρ is the maximal resistivity just over the PTC transition and ρ_0 is the resistivity at room temperature. The effect of the alloy volume fraction on the PTC intensity is shown in Figure 3(a). As shown in Figure 3(a), the PTC intensity increases with the increasing volume fraction. This phenomenon is different from the normal carbon

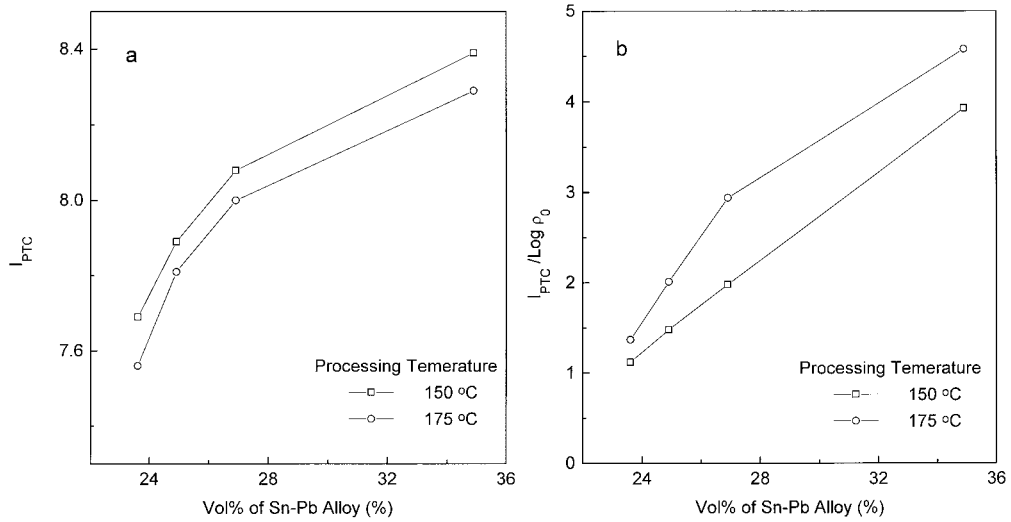

Figure 3 (a) PTC intensity and (b) $I_{PTC}/\log \rho_0$ as functions of the alloy volume fraction for the composites processed at various temperatures.

black-loaded polyethylene whose PTC intensity decreases with increase of the carbon black concentration over the critical threshold.[12]

To weight the proportionality of low room-temperature resistivity and high PTC intensity, another parameter is defined:

$$\frac{I_{PTC}}{\log \rho_0} = \frac{\log \rho - \log \rho_0}{\log \rho_0} \tag{2}$$

From Figure 3(b), where I_{PTC}/ρ_0 is plotted against the alloy volume fraction, it can be seen that $I_{PTC}/\log \rho_0$ increases with the increasing volume fraction, indicating that low room-temperature resistivity and high PTC intensity can be gained simultaneously only by increasing the alloy loading. It can also be seen in Figure 3 that the higher processing temperature brings about the lower PTC intensity and higher $I_{PTC}/\log \rho_0$.

Dispersion of Alloy Particles

The two main factors which affect the resistivity of the composites are the volume fraction and the dispersion of the conductive filler. As the alloy loading is fixed and the PS matrix (amorphous polymer) exhibits no abrupt change of thermal expansion (which can induce the change of the real alloy volume fraction) during the PTC transition in our study, the PTC effect observed may be caused by the dispersion change of the alloy particles in the composites.

As the particle dispersion in composites can be characterized by the spatial arrangement of particles (point pattern), the digital image analysis (DIA) developed by Tanaka et al.[8] was applied in our study. The Sn distribution (X-ray map) of three differently treated composites (26.9 vol % Sn–Pb alloy), which were as-prepared, cooled down gradually from 240°C, and quenched in an ice/water mixture from 240°C, respectively, were detected and imaged by EDAX first (Fig. 4).

To study the Sn element distribution, the three X-ray maps are converted to the corresponding point patterns (the top three patterns in Fig. 5). The corresponding Voronoi polygons and Delauney triangles drawn according to ref. 8 are also shown in Figure 5 (to make the patterns clearer, only the right bottom parts of each pattern are shown). The cluster of points is clearly seen, which is common in conductive composites.

There are a few kinds of special functions which give us information on the spatial distribution of points.[8] Two of the functions, that is, the so-called p function and q function, were used in our study. The p function is a cumulative distribution function of the distance between the random point and the nearest object r_1, and it is defined by

$$p(t) = Pr(r_1 < t) \tag{3}$$

where Pr ( ) is the probability. The q function is a cumulative distribution function of the distance

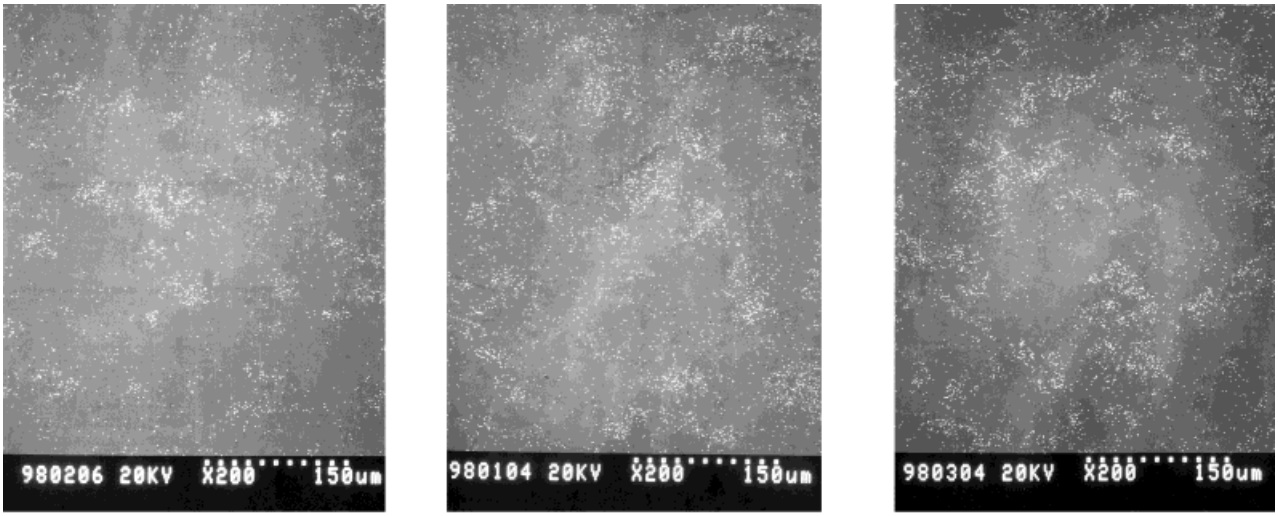

Figure 4 Sn X-ray maps for composites (a) quenched in ice/water mixture from 240°C, (b) cooled gradually from 240°C, and (c) as-prepared.

between two nearest-neighbor points r_2 and is defined by

$$q(t) = Pr(r_2 < t) \tag{4}$$

The behavior of $p(t)$ and $q(t)$ for the pattern is shown in Figure 6, where t is defined as $t = r/r_0$, and $r_0 = (S/N)^{1/2}$ (where S is the total area and N is the number of the points). Both $p(t)$ and $q(t)$ increase with increasing r/r_0; however, the increase of $p(t)$ is sharp and that of $q(t)$ is a little flat, which is characteristic of the aggregated system with many clusters.[8] From Figure 6, it can also be seen that the deviation between $p(t)$ and $q(t)$ for the composite quenched from 240°C is less than that of the other two composites, indicating that the Sn element in this situation is less clustered.

Through the study of the Sn element distribution, the change of alloy particle dispersion in the composites during heating is known. In the composite as-prepared, the alloy particles form clusters (see curves 3 and 3′ in Fig. 6), which is the essential factor of the establishment of a conductive network, and the resistivity is very low. When the temperature increases over the melting point of the alloy, the alloy particles tend to be dispersed more uniformly (see curves 1 and 1′ in Fig. 6). Note that only small changes in the relative position of neighboring aggregates would suffice to bring about an appreciable change in conductivity[13]; therefore, the resistivity increases abruptly and the PTC effect appears. However, when the composites are cooled gradually to room temperature after the temperature run, the clusters are reestablished into the initial stage to some degree (see curves 2 and 2′ in Fig. 6) and the reversibility of the PTC effect is achieved.

Morphology of Alloy Particles in Composites

It has been known that the PTC effect is directly caused by the dispersion change of alloy particles in composites; however, the possible origin of the dispersion change is abundant, such as the particle morphology, interface energy, and processing conditions. The morphology of alloy particles (the most important aspect of the particle morphology, which affects the resistivity, is the particle size) was studied first, and the SEM image of the composites loaded with the Sn–Pb alloy (26.9 vol % Sn–Pb alloy) is shown in Figure 7. The alloy particles in the composites as-prepared are aggregates of small original particles [Fig. 7(a)]. At the same time, the alloy particles in the composites, which are quenched in an ice/water mixture from 240°C after the temperature run [Fig. 7(b)], remain in the form of aggregates of small particles. Therefore, the aggregates do not fuse into large particles and the particle size of the alloy does not change when the temperature reaches the melting point of the alloy. As a result, the dispersion change is not caused by the morphology change of the alloy particles.

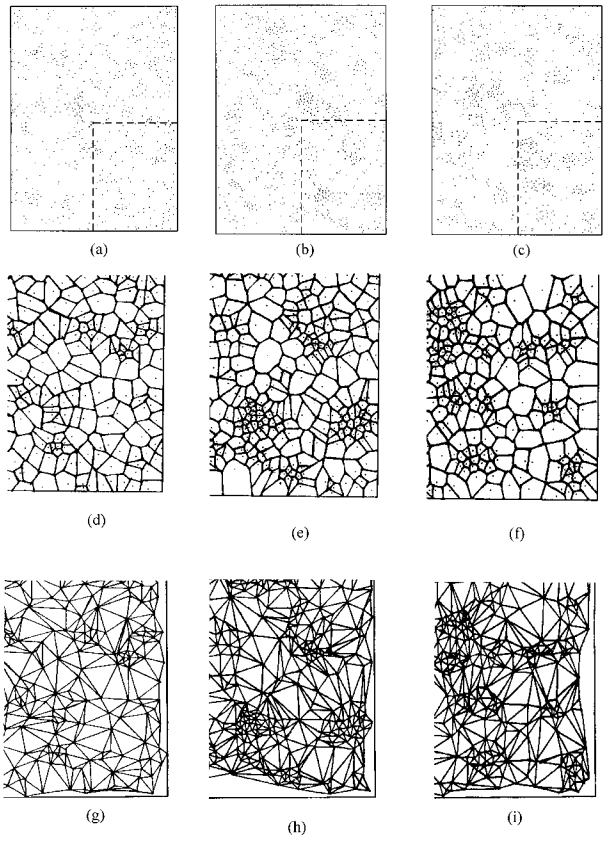

Figure 5 Point patterns for the composites (a) quenched in ice/water mixture from 240°C, (b) cooled gradually from 240°C, and (c) as-prepared; (d–f) the three corresponding Voronoi polygons; (g–i) Delauney triangles.

Possible Mechanism

As the dispersion change is not caused by change of the alloy particle morphology, there must be some abrupt change of other aspects which are the origin of the PTC effect. It is noticed that the surface energy of the solid near the melting point is about 10–20% higher than that of the corresponding liquid.[14] Therefore, when the temperature reaches the melting point, the surface energy of the alloy is reduced, approaching that of the PS to some extent, and the wettability of the alloy particles for PS is then improved. Although such improvement is not very large, its effect on the resistivity is apparent as the property of the composites is very sensitive to the wettability of the filler for the polymer matrix.[15] When the wettability increases, the PS will have the trend to "enwrap" the alloy particles, and the particles are then better dispersed. As a result, the PTC transition at the melting point of the alloy is caused by the surface energy change of the alloy from the thermodynamic point of view.

The effect of temperature on the viscosity of the composites is shown in Figure 8. As shown in Figure 8, the viscosity of the composites decreases with increase of the temperature at the whole temperature range of interest. The more important thing is that the viscosity decreases sharply at the melting point of the alloy and the sharp drop of the viscosity facilitates the movement of the alloy particles. As a result, the sudden change of the surface energy of the alloy at the melting point provides the possibility of thermodynamics for the dispersion change,[16] while the sharp decrease of the viscosity promotes the dispersion change from the dynamics point of view.

In short, the possible mechanism is that the Sn–Pb alloy melts when the temperature reaches the melting point, and the surface energy decreases abruptly. As a result, the wettability of the alloy for PS will be improved, and the alloy particles are then dispersed more uniformly. The sharp decrease of the viscosity promotes that process. Then, the breakup of conductive networks appears, and the resistivity increases suddenly at the melting point of the alloy, that is, the PTC transition appears. As the surface energy can recover itself when the temperature decreases, the breakup of conductive networks is reversible.

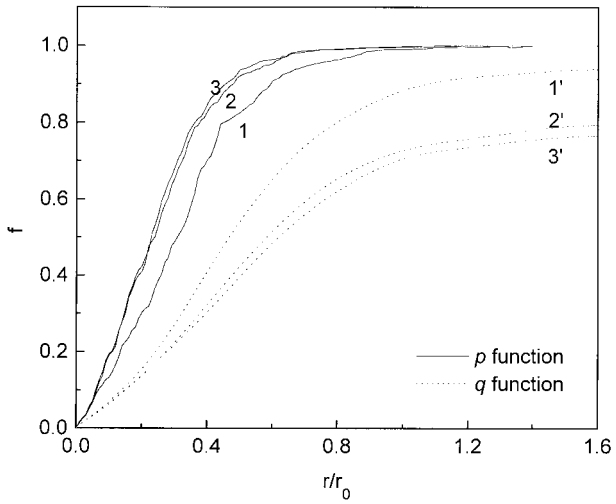

Figure 6 p and q functions for the point pattern of composites (1, 1′) quenched in ice/water mixture from 240°C, (2, 2′) cooled gradually from 240°C, and (3, 3′) as-prepared.

Figure 7 Scanning electron micrographs for the fracture surfaces of composites (a) as-prepared and (b) quenched in ice/water mixture from 240°C.

CONCLUSIONS

The resistivity–temperature behavior of the Sn–Pb alloy-loaded PS was studied. It was observed that the Sn–Pb alloy-loaded PS is a distinctive PTC material, and the origin of the PTC effect is the state change of the alloy fillers instead of other changes of the polymer matrix. The PTC effect of the Sn–Pb alloy-loaded PS has many advantages: (1) high PTC intensity, (2) abrupt PTC transition behavior, and (3) adjustable PTC transition temperature by easily selecting the filler alloys with different melting points.

The effect of temperature on the morphology and dispersion of the alloy particles in composites was also studied. The dispersion of the alloy particles in composites varies dramatically when the temperature reaches the melting point of the alloy and becomes the direct cause of the PTC effect. The morphology of the alloy particles does not change, while the surface energy of the alloy and the viscosity of the composites decrease dramatically as the alloy melts. As a result, the origin of the PTC effect is the abrupt decrease of the alloy surface energy from the thermodynamics point of view and the sharp drop of the viscosity of the composites from the dynamics point of view.

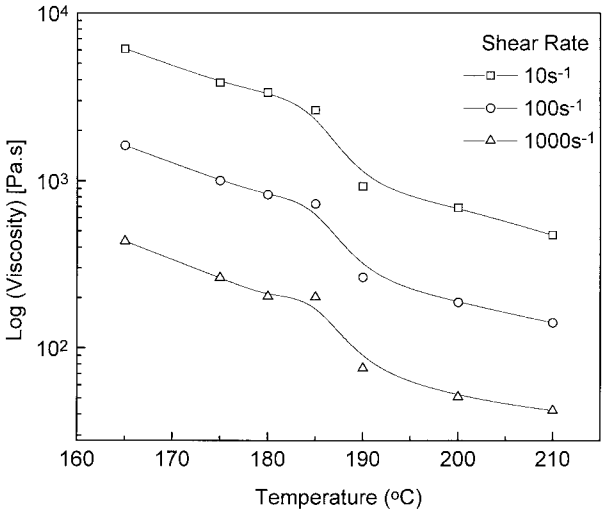

Figure 8 Viscosity of Sn–Pb alloy-loaded PS composite (35 vol % Sn–Pb alloy) as a function of the temperature at various shear rates.

The authors wish to express their gratitude to the National Nature Science Foundation of China (NNSFC, Grant 59683003) for financing the project. Thanks are also due to the Institute of Powder Metallurgy of the Zhongnan Technology University of China for providing the Sn–Pb alloy free of charge.

REFERENCES

1. Malliaris, A.; Turner, D. T. J Appl Phys 1971, 42, 614.
2. Matsushia, R.; Senna, M.; Kuno, H. J Mater Sci 1977, 12, 509.

3. Nicodemo, L.; Nicolais, L.; Romeo, G.; Scufora, E. Polym Eng Sci 1978, 18, 293.
4. Bhattacharya, S. K.; Basu, S.; De, S. K. Composites 1978, July, 177.
5. Lyons, A. M. Polym Eng Sci 1991, 31, 445.
6. Li, L.; Chung, D. D. L. Polym Compos 1993, 14, 361.
7. Toshiba Chemical Products, Jpn Patent 56 220 714, Dec. 1983.
8. Tanaka, H.; Hayashi, T.; Nishi, T. J Appl Phys 1989, 65, 4480.
9. Wang, B. X.; Yi, X. S.; Pan, Y.; Shan H. F. J Mater Sci. Lett 1997, 16, 2005.
10. Meyer, J. Polym Eng Sci 1973, 13, 462.
11. Ohe, K.; Nitio, Y. Jpn J Appl Phys 1971, 10, 99.
12. Narkis, M. Polym Eng Sci 1978, 18, 649.
13. Medalia, A. I. Rubb Chem Technol 1985, 59, 432.
14. Cui, G. W. In Surface and Interface; Gui, G. W., Ed., Tsinghua: Peking, 1990; p 57.
15. Lux, F. J Mater Sci 1993, 28, 285.
16. Miyasaka, K.; Watanabe, K.; Jojima, E. J Mater Sci 1982, 17, 1610.